Arabidopsis Capping Protein (AtCP) Is a Heterodimer That Regulates Assembly at the Barbed Ends of Actin Filaments*

Shanjin Huang‡, Laurent Blanchoin§¶, David R. Kovar‖**, and Christopher J. Staiger‡ ‡‡

From the ‡Department of Biological Sciences and Purdue Motility Group, Purdue University, West Lafayette, Indiana 47907-2064, §Laboratoire de Physiologie Cellulaire Végétale, Commissariat à l'Energie Atomique (CEA)/CNRS/Université Joseph Fourier, CEA F38054 Grenoble, France, and ‖Department of Molecular, Cellular and Developmental Biology, Yale University, New Haven, Connecticut 06511

The precise regulation of actin filament polymerization and depolymerization is essential for many cellular processes and is choreographed by a multitude of actin-binding proteins (ABPs). In higher plants the number of well characterized ABPs is quite limited, and some evidence points to significant differences in the biochemical properties of apparently conserved proteins. Here we provide the first evidence for the existence and biochemical properties of a heterodimeric capping protein from *Arabidopsis thaliana* (AtCP). The purified recombinant protein binds to actin filament barbed ends with K_d values of 12–24 nM, as assayed both kinetically and at steady state. AtCP prevents the addition of profilin actin to barbed ends during a seeded elongation reaction and suppresses dilution-mediated depolymerization. It does not, however, sever actin filaments and does not have a preference for the source of actin. During assembly from Mg-ATP-actin monomers, AtCP eliminates the initial lag period for actin polymerization and increases the maximum rate of polymerization. Indeed, the efficiency of actin nucleation of 0.042 pointed ends created per AtCP polypeptide compares favorably with mouse CapZ, which has a maximal nucleation of 0.17 pointed ends per CapZ polypeptide. AtCP activity is not affected by calcium but is sensitive to phosphatidylinositol 4,5-bisphosphate. We propose that AtCP is a major regulator of actin dynamics in plant cells that, together with abundant profilin, is responsible for maintaining a large pool of actin subunits and a surprisingly small population of F-actin.

The cytoskeleton in plant cells comprises a dynamic network of actin filaments, microtubules, and accessory proteins that powers cytoplasmic streaming, responds rapidly to prevent fungal attack, patterns the deposition of cellulosic wall polymers, and shapes cellular morphogenesis by choreographing exo- and endocytotic vesicle traffic. Understanding how the cytoskeleton is organized, how it responds to extrinsic and intrinsic cues, and how dynamics are regulated are central questions in plant biology (1). To date less than a dozen of the more than 70 classes of actin-binding proteins (ABPs)[1] found in eukaryotic cells (2, 3) have been isolated and characterized from plants. Particularly well studied are members of the profilin, ADF/cofilin, fimbrin, villin, EF-1α, and myosin families (4, 5). Although the general properties of ABPs are often conserved across kingdoms, important differences highlight the need to examine in detail the functional properties of proteins from divergent organisms. For example, *Chlamydomonas* profilin binds extremely poorly to one of the major known ligands (poly-L-proline) and inhibits nucleotide exchange on actin (6), and phylogenetically unique classes of plant myosins are the fastest molecular motors on the planet (7). Based on genome sequencing, many classes of ABP are missing from higher plants, including α-actinin, spectrin, tropomyosin, WASp, and coronin (4, 8). One intriguing possibility is that multiple isoforms from a small subset of ABP families have evolved divergent functions to accommodate all of the known structural and regulatory cytoskeletal functions (4, 9). Limited biochemical evidence for this hypothesis, based mainly on work with plant profilins and ADF/cofilins, is available (10, 11).

Precise coordination of actin filament polymerization and turnover is essential to drive cellular motility, to propel bacterial and viral pathogens intracellularly, and to form organized cytoplasmic networks (3, 12, 13). A central feature of all these processes is regulation of the number and availability of filament ends. For example, cloud-like networks of dendritically nucleated actin filaments formed on Arp2/3-coated beads *in vitro* are converted to filopodia-like bundles in the absence of capping protein (14). Several classes of ABPs are known to control filament ends *in vitro* and *in vivo* (2, 15). Capping proteins regulate the addition and loss of subunits from either the barbed (plus) or pointed (minus) ends of filaments. Nucleating factors mimic the seed required for efficient actin polymerization and create new barbed ends for assembly. Severing proteins break the filament backbone and thereby create one or two new ends for subunit loss or addition. And, dynamizing factors shuttle subunits onto or from filament ends. Surprisingly, there is no direct evidence for capping proteins in plant systems.

Capping protein (CP; also known as CapZ or β-actinin from vertebrate muscle and cap32/34 from *Dictyostelium*) is a het-

[1] The abbreviations used are: ABP, actin-binding protein; AtCP, *A. thaliana* capping protein; CP, capping protein; G-actin, globular or monomeric actin; F-actin, filamentous actin; PtdIns(4,5)P₂, phosphatidylinositol-4,5-bisphosphate; DTT, dithiothreitol.

erodimeric protein complex composed of α (32–36 kDa) and β (28–32 kDa) subunits (16–18). Ample biochemical, cytological, and genetic evidence for CP from yeasts, vertebrates, flies, and worms supports the assertion that CP is a major regulator of filament assembly in many organisms. Indeed, CP is one of three ABPs that precisely choreograph actin polymerization and organization to generate "comet-tail" motility *in vitro* (12). Biomimetic systems that reproduce *Listeria* motility demonstrate that varying [CP] affects the shape and organization of actin filament comet tails (19) and modulates the velocity of movement (20). At a biochemical level CP binds with high affinity (K_d values of 0.06–5 nM) to filament barbed ends and prevents subunit loss and addition from that end. In the presence of saturating amounts of the monomer (G) actin-protein binding profilin, CP prevents subunit loss at barbed ends, and addition at both ends is blocked. A recent crystal structure of chicken muscle CapZ ($\alpha1\beta1$ heterodimer) suggests how the heterodimer may interact with two actin subunits simultaneously and thereby act as a seed for further filament assembly (21). CP is regulated by phosphoinositide lipids that are implicated in signaling (22–24) and probably modulates actin polymerization at or near cellular membranes (25, 26). Its activity or cellular location may also be modulated by interaction with other proteins and protein complexes, including twinfilin (27), the myosin I and Arp2/3-interacting protein CARMIL (28), V-1 protein (29), and Arp1 minifilaments that are part of the dynactin complex (30). In this study we report first evidence for the existence and biochemical activities of CP from a higher plant. Both subunits for heterodimeric CP from the model organism, *Arabidopsis thaliana*, were cloned, and the recombinant proteins were co-expressed in bacteria for biochemical and microscopic examination of function.

EXPERIMENTAL PROCEDURES

Expression and Purification of Heterodimeric CP—cDNAs encoding *A. thaliana* F-actin-capping protein α and β subunits (AtCPA and AtCPB) were amplified by PCR from a size-fractionated root cDNA library (CD4–16; *Arabidopsis* Stock Center, Ohio State University). Oligonucleotide primers were synthesized based on the predicted mRNA sequences available in the EMBL and GenBank™ databases (accessions numbers AJ001855 and AC012654, respectively). The primers for amplification of AtCPA were 5′-TAACATATGGCGGACGAAGAAGATGAG-3′ (the forward oligonucleotide) containing the initiation codon and an NdeI site (underlined), and 5′-CCCAAGCTTTCACTTGCCAAGTCCAAGTTC-3′ (the reverse oligonucleotide) containing the stop codon and a HindIII site (underlined). The primers for amplification of AtCPB were 5′-CTCGAGTCAGGTGTCAGGCAATCTCA-3′ (the reverse oligonucleotide) containing the stop codon and an XhoI site (underlined), and 5′-ATACATATGGGAGGCAGCTTTGGGAC-3′ (the forward oligonucleotide) containing the initiation codon and an NdeI site (underlined). The amplified products were A-tailed and cloned into the pGEM-T vector. The sequence of the cloned cDNAs was confirmed by sequence analysis.

For expression of *Arabidopsis* capping protein α and β subunits in *Escherichia coli*, the strategy of Soeno *et al.* (31) was used. Construct pET23a-A was created by cloning the full-length cDNA of AtCPA into pET23a vector prepared with NdeI and HindIII. Construct pET23a-B was created by cloning the full-length cDNA of AtCPB into pET23a prepared with NdeI and XhoI. A DNA fragment of ~1.1 kilobases, including the entire coding sequence for AtCPB preceded by the T7 RNA polymerase promoter at its 5′-end and followed by T7 terminator sequence at the 3′-end, was excised from pET23a-B with HaeII and BglII. This fragment was blunt-ended with T4 polymerase and ligated into the pET23a-A vector prepared with MscI. The resulting expression plasmid was designated pET-23a-AB.

The pET-23a-AB construct was transformed into strain BL21 (DE3) of *E. coli*, and cells were grown overnight at 37 °C. After subculturing into fresh media, cells were grown at 37 °C for 2 h, then induced for 3 h at 37 °C with the addition of 1 mM isopropyl β-D-thiogalactopyranoside. Cells were collected by centrifugation and resuspended in 50 mM Tris-HCl, pH 8.0, supplemented with a 1:200 dilution of protease inhibitors from a stock solution (32) and sonicated. The sonicate was clarified at

46,000 × *g*. The AtCP complex was precipitated from the supernatant with $(NH_4)_2SO_4$ at 45–60% saturation. The pellet was dissolved in solution A containing 175 mM KCl, 1 mM DTT, 0.01% NaN_3, 10 mM Tris-HCl, pH 7.0, 1:200 dilution of protease inhibitors and dialyzed against the same solution at 4 °C. The dialyzed protein was applied to a DEAE-Sephacel column pre-equilibrated with solution A, and bound proteins were eluted with a linear gradient of KCl (175–350 mM). Fractions containing AtCP were pooled and dialyzed against solution B containing 500 mM KCl, 1 mM DTT, 0.01% NaN_3, 40 mM potassium phosphate buffer, pH 7.0, and applied to a hydroxylapatite column equilibrated with solution B. The protein was eluted with a linear gradient (40–150 mM) of potassium phosphate buffer, pH 7.0. The protein was dialyzed against solution C containing 250 mM KCl, 1 mM DTT, 0.01% NaN_3, 10 mM Tris-HCl, pH 8.0, supplemented with 1:200 protease inhibitors and applied to a Q-Sepharose column. Bound protein was eluted with a linear gradient of KCl (250–500 mM). The purified AtCP was dialyzed against Buffer G (2 mM Tris-HCl, pH 8.0, 0.01% NaN_3, 0.2 mM CaCl_2, 0.2 mM ATP, 0.2 mM DTT), separated into aliquots, frozen in liquid nitrogen, and stored at −80 °C. The protein was clarified further by centrifugation at 200,000 × *g* for 1 h before use. Recombinant mouse capping protein ($\alpha1\beta2$), hereafter referred to as mouse CapZ or CapZ, was purified according to Palmgren *et al.* (27). Capping protein concentrations were determined with the Bradford assay (Bio-Rad) with bovine serum albumin as a standard.

Polyclonal Antibody Production—Purified AtCPA and AtCPB were used to elicit polyclonal antisera production in New Zealand White rabbits according to standard procedures as described previously (33). The proteins for antibody production were expressed separately as glutathione *S*-transferase fusion proteins, digested with thrombin, and purified according to Kovar *et al.* (34). The strategy for making pGEX-KG-A and pGEX-KG-B expression plasmids was similar to the pET-23a construct described above. Blot affinity-purified antibodies were prepared essentially according to Tang (35). AtCPA and AtCPB were separated on 15% SDS-PAGE gels and transferred to nitrocellulose membrane. Horizontal strips containing AtCPA and AtCPB were excised and blocked for 1 h in Tris-buffered saline containing 3% (w/v) bovine serum albumin and 0.5% (v/v) Tween 20. Individual strips were incubated overnight at room temperature in rabbit serum diluted 1:50 with Tris-buffered saline containing 0.5% (v/v) Tween 20. The nitrocellulose was washed 3 times with 10 ml of Tris-buffered saline, Tween 20 for 5 min with gentle agitation to remove unbound antibodies. Bound antibodies were eluted with 2 ml of glycine elution buffer (0.1 M glycine-HCl, pH 2.5, 0.5 M NaCl, 0.05% Tween 20) for 3 min on ice with gentle mixing. Eluted antibodies were transferred immediately to a test tube containing 0.3 ml of 1 M Tris, pH 8.0, for neutralization. Elution and neutralization were repeated once for each nitrocellulose strip followed by a 2-ml Tris-buffered saline, Tween 20 rinse. The two eluates and the rinse were combined and supplemented with 0.75 ml of 10% (w/v) bovine serum albumin and 75 μl of 5% NaN_3, separated into aliquots, and stored at −80 °C. This antibody eluate, at a 1:100 dilution, was used for Western blotting.

Actin Purification—Actin was purified from rabbit skeletal muscle acetone powder (36), and monomeric Ca-ATP-actin was purified by Sephacryl S-300 chromatography (37) in G buffer (5 mM Tris-HCl, pH 8, 0.2 mM ATP, 0.1 mM CaCl_2, 0.5 mM DTT, 0.1 mM azide). Actin was labeled on Cys-374 with pyrene iodoacetamide (37).

Maize pollen actin was purified as described previously (32) with minor modifications. A 5–10-g sample of frozen pollen was ground with a mortar and pestle for 25 min in 50 ml of buffer A (10 mM Tris-HCl, pH 8.5, 0.5 mM CaCl_2, 0.01% NaN_3, 50 mM NaF, 30 mM NaPP_i, 0.4 mM ATP, 0.5 mM DTT, 0.5 mM phenylmethylsulfonyl fluoride, and 1:200 protease inhibitor mixture). During the grinding a total of 25 mg of recombinant human profilin I was added in 3 steps. After sonication (five 30-s bursts) and two clarification steps (32), the extract was supplemented with 0.4 mM ATP. For experiments in this study the actin that eluted from poly-L-proline-Sepharose with 1 M KCl followed by a cycle of assembly/disassembly was used. The protein concentration of vertebrate or plant actin solutions was determined by spectrometry assuming an A_{290} for a 1 mg/ml solution of 0.63 (10, 38).

Critical Concentration Determination—The critical concentration (C_c) for actin polymerization was determined as described by Brenner and Korn (39). Increasing concentrations of 5% pyrene-labeled actin were polymerized in 1× KMEI (50 mM KCl, 1 mM MgCl_2, 1 mM EGTA, and 10 mM imidazole-HCl, pH 7.0) in the absence or presence of 100 nM AtCP or 100 nM CapZ for 16 h at room temperature in the dark. Fluorescence measurement was performed at room temperature using an PTI Alphascan spectrofluorometer (Photon Technology International, South Brunswick, NJ) with excitation set at 365 nm and emis-

sion detected at 407 nm. Linear best fit of the data, plotted as arbitrary fluorescence units *versus* actin concentration, was used to determine the intercept with the *x* axis.

Measurement of Nucleating Activity—Actin nucleation was carried out essentially as described by Schafer *et al.* (24). To test the nucleating activity of AtCP and CapZ, we measured their effect on the initial phase of actin polymerization. Monomeric actin at 2 μM (5% pyrene-labeled) was incubated with AtCP or CapZ for 5 min in Buffer G. Fluorescence of pyrene-actin was monitored after the addition of ¹⁄₁₀ volume of 10× KMEI. The number of ends (*N*) generated during the nucleation reaction was calculated from the slope of the polymerization curves at half polymerization according to Equation 1,

$$\text{Slope} = k_+ A N - k_- N \qquad (\text{Eq. 1})$$

where k_+ is the association rate constant at the pointed ends (1.3 μM^{-1} s^{-1}) (40), k_- is the dissociation rate constant (0.8 s^{-1}), and *A* is the concentration of actin monomers. The efficiency of nucleation by capping proteins is calculated from the ratio between the number of ends (*N*) generated during the polymerization and the concentration of AtCP or CapZ used during the experiments.

Dynamics of Actin Filament Depolymerization—F-actin at 5 μM (40–50% pyrene-labeled) was mixed with varying concentrations of AtCP, or CapZ, incubated at room temperature for 5 min, and diluted 25-fold into Buffer G at room temperature. The decrease in pyrene fluorescence accompanying actin depolymerization was monitored for 600 s after dilution. The affinity of capping proteins for the barbed ends of actin filaments was determined by the variation of the initial rate of depolymerization as a function of the concentration of capping protein using Equation 2,

$$Vi = Vif + (Vib - Vif)$$

$$\left(\frac{(K_d + [\text{ends}] + [CP]) - \sqrt{(K_d + [\text{ends}] + [CP])^2 - (4[\text{ends}][CP])}}{2[\text{ends}]} \right)$$

$$(\text{Eq. 2})$$

where Vi is the observed rate of depolymerization, Vif is the rate of disassembly when all barbed ends are free, Vib is the rate of depolymerization when all barbed ends are capped, [ends] is the concentration of barbed ends, and [CP] is the concentration of capping protein. The data were modeled with Kaleidagraph v3.6 software (Synergy Software, Reading, PA).

Elongation Assay to Determine the Affinity of Capping Proteins for Actin Filaments—Various concentrations of AtCP or CapZ were incubated with 0.4 μM preformed actin filaments in KMEI for 5 min at room temperature. The reaction mixtures were supplemented with 1 μM G-actin (5% pyrene-labeled) saturated by 4 μM human profilin 1 to initiate actin elongation at barbed ends. Under these conditions the initial rate of elongation depends on the number of available barbed ends (*N*), according to Equation 3,

$$\text{Rate} = k_+ A N - k_- N \qquad (\text{Eq. 3})$$

where k_+ is the association rate constant (10 μM^{-1} s^{-1}), k_- is the dissociation rate constant (1 s^{-1}), and *A* is the concentration of actin monomers bound to profilin. Under these conditions the initial rate of elongation decreased as filament barbed ends were saturated by capping protein. The affinity of capping protein for the barbed ends of actin filaments was determined by the variation of the initial rate of elongation as a function of the concentration of capping protein using Equation 2 as above but where Vi is the observed rate of elongation, Vif is the rate of elongation when all barbed ends are free, Vib is the rate of elongation when all barbed ends are capped, [ends] is the concentration of barbed ends, and [CP] is the concentration of capping protein.

The effect of calcium on affinity of AtCP for filament barbed ends was determined with reactions in which the concentration of EGTA was kept constant at 1.12 mM, and variable amounts of Ca^{2+} added to obtain free Ca^{2+} concentrations of 200 nM and 2, 20, and 200 μM. Free Ca^{2+} was calculated with "EGTA" software by Petesmif (P. M. Smith, The University of Liverpool), available at www.liv.ac.uk/luds/people/cds/bds/pms/cal.htm. Apparent binding constants for association of AtCP with filament barbed ends were calculated from one representative experiment using the modified Equation 2, as above.

To test the effect of phospholipids on CP activity, elongation and depolymerization assays were performed in the presence of varying concentrations of phosphatidylinositol 4,5-bisphosphate (PtdIns(4,5)P₂; Sigma) micelles. Experimental conditions for measuring changes in

F-actin levels were as described above, except that CP was preincubated with different amounts of PtdIns(4,5)P₂ for 5 min on ice before the addition of pyrene-actin. Micelles were prepared from a stock solution (1 mg/ml or 915 μM) by sonication in distilled water for 5 min at room temperature, as described previously (6).

Determination of the Affinity of CP for F-actin at Steady State—K_d values were also determined by measuring the effect of capping protein on steady-state F-actin levels (41). The effect of AtCP and CapZ on the steady-state actin filament concentration for rabbit muscle actin was determined by incubation of 1 μM actin (5% pyrene-labeled) in KMEI with varying concentrations of AtCP and CapZ. Samples were incubated for 24 h at room temperature, and fluorescence was determined with the fluorometer. The fluorescence of pyrene actin was plotted *versus* the log of the capping protein concentration. The K_d for capping protein binding to actin was determined as the amount of capping protein that changes the critical concentration by 50% (42).

Fluorescence Microscopy of Actin Filaments—To visualize actin filaments generated during nucleation, actin at 4 μM alone or together with CapZ or AtCP were polymerized in 50 mM KCl, 2 mM MgCl₂, 1 mM EGTA, 0.2 mM ATP, 0.2 mM CaCl₂, 0.5 mM DTT, 3 mM NaN₃, and 10 mM imidazole, pH 7, at 25 °C for 30 min and labeled with rhodamine-phalloidin during polymerization (43). The polymerized F-actin was diluted to 10 nM in fluorescence buffer containing 10 mM imidazole, pH 7.0, 50 mM KCl, 1 mM MgCl₂, 100 mM DTT, 100 μg/ml glucose oxidase, 15 mg/ml glucose, 20 μg/ml catalase, 0.5% methylcellulose. A dilute sample of 3 μl was applied to a 22 × 22-mm coverslip coated with poly-L-lysine (0.01%). Actin filaments were observed by epifluorescence illumination under a Nikon Microphot SA microscope equipped with a 60×, 1.4 NA Planapo objective, and digital images were collected with a Hamamatsu ORCA-ER 12-bit CCD camera using Metamorph 6.0 software. In the elongation assay using microscopy, actin seeds stabilized by rhodamine phalloidin were elongated by actin monomers for 15 min in the presence of phalloidin conjugated to Alexa-488 (Molecular Probes, Eugene OR) to stabilize the new filaments (43). Samples were prepared by dilution and application to a coverslip. Annealing experiments were analyzed by wide-field fluorescence microscopy or with a total internal reflection fluorescence microscope (Nikon) using laser excitation at 488 or 543 nm and the digital imaging system described above.

RESULTS

Identification of Plant Capping Protein—*A. thaliana* cDNA sequences for putative α and β subunits of heterodimeric capping protein were identified in current databases. The full-length cDNA for *AtCPA* (AJ001855) encodes a predicted polypeptide of 308 amino acids (Fig. 1*A*) with a molecular mass of ~35 kDa and pI of 4.58. *AtCPB* is deduced from genomic sequence information obtained from BAC clone F14023 (AC012654). The β subunit is predicted to be 256 amino acids (Fig. 1*B*) with a molecular mass of 28.9 kDa and pI of 4.55 and is supported by a single Expressed Sequence Tag (AV560772). When compared with capping protein α and β subunits from different organisms, the β subunit of AtCP appears to be more highly conserved. AtCPB shares 40–51% amino acid sequence identity with β-subunits from vertebrates and yeasts, whereas AtCPA shares just 25–30% with α-subunits. Each subunit appears to be encoded by a single gene in *Arabidopsis*. The rice (*Oryza sativa cv. japonica*) genome also contains a putative α-subunit of capping protein (OsCPA) that shares 61% identity and 77% similarity with AtCPA. OsCPA is predicted to be 297 amino acids (Fig. 1*A*) with a molecular mass of 33.1 kDa and pI of 4.83. No obvious candidates for a rice β-subunit of capping protein were found, however. Mutagenesis studies and the recent crystal structure of chicken muscle CapZ α1/β1 heterodimer implicate the C-terminal regions of both subunits in binding to F-actin (21, 44, 45). It is noteworthy that these regions are quite poorly conserved in AtCPA and AtCPB. We amplified the coding regions for the α and β subunits, AtCPA and AtCPB, from a size-fractionated *Arabidopsis* root library and verified the sequences present in the database.

Generation of Recombinant AtCP—To analyze the functional properties of plant capping protein, both AtCP subunits were
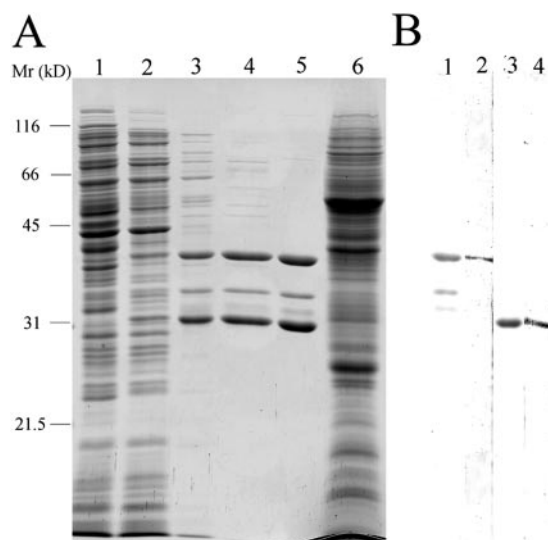
A

	1
AtCPA	MADEEDELLET ELSYD QKKE IAKWFFLNA PAGE INYVAKD LKAVLSDEEVYNEAAME AFPVYN KTHMICLEMPSGAGD VI
OsCPA	MSDGEE - - - - - - - - - - KRE IAVWFLSNA PAGE IHYVRALLDEAVYEAAAAE AFPEH NKAHLVALKTDPRSGD II
Chicken A1	MADFEDRVSDE E - - - - - KVR IAAKFITHA PPGE FNEVFNDVRLLLNNDNLLREGAAHA FAQYNMDQFTPVKIEGYDDQ VL
S. cerevisiae	MS SSK - - - - - - - - - - - FEEV IKINDS PPGE LREVYDDLIKITSENS - - KNTILDAI ENVQNCIPIEVNG - - NS VI
S. pombe	MEKEA IYKLIRES PPGE VNQVVHDIRDIGLSD - - - EEAIHEQLKLY HEDYNSSVSISD-DEKVI

AtCPA	VSSYSEINENEYL DPR TAQVAIVD HVKQICTKVRP ANDEE LPSLYIEEYRYALD-AEIQRYVSES YPKGMSAVNCVKGK GD
OsCPA	ITTYGELDKNNYL DPR TAQVATVDH IKQKCTKLRP AADEE LPSAYIEDFRSALD-VELSKYVGEAYPKGVCAVYCTSGK GD
Chicken A1	ITEHGDLGNGRFL DPR NKISFKFDHLRKEASDPQPE-D - - - TESALKQWRDACD-SALRAYVKDHYPNGFCTVY - - -GK S
S. cerevisiae	ISKYNKE-GAKFF DPV NSVIFSVNHLERKGLDIE PY - - - EFTHAKIEKGQLKEL HDKHLLQSFPGDVSFAVYP - -V P
S. pombe	ISADNRLEGNRYY DQV LQKSFTINYETMEAENVEDY - - - - - - TEAIKIPDEIV-KQIKKVASDHYLSDVTFGIIK - -KS

AtCPA	NEGPGS DFE LVVI IT AMRLS PQNF CNGS WRS VWNIDFQDESQVLDIKKGK LQVGAH YFEEGNV LKDFQDST IFQSAD
OsCPA	IEGPGV DFR FAAVI SAAKRS PQNF CNGN WRS IWTLEFIDGLQLVEIKGK IQVGAH YFEEGNV QLDTNIDCKDST ILQSPE
Chicken A1	IDGQQ - - - TIIACI ESHQFQPK NWN FWNG HWRS EWKFTITPPTAQVAAVLKIQVHY YEDGNVQLVSHKDIQDST VSQVSSDV
S. cerevisiae	EFISK - - - - ISI I IVSTKVNP NNF WNG HWRS SYIYDLETRE - - LSGQISTQV HYYEDGNVSFQSGKDINQSN VDDV -
S. pombe	DEVES - - - - FTIVLVSSKYNPKNY WNG S WRC ICNYNVSEKK - - LEGRSHIRV HYYEDGNWLDASRPISATVEETS - -

		308
AtCPA	DC A IAIANI I RHH ETEYLASLEVAYSK LP DNT FKD LRRK LPVTR LFPWQNTLQFSLTREVEKELGL GK
OsCPA	EC A VSITNI I RHH ESEYLSSLEESYMN LS DAT FKD LRRK LPVTR TLFPWHNTLALSLTRDLTKELAI GK
Chicken A1	QT A KEFIKI I ENA ENEYVQTMS DT TFKA LRRQ LPVTR TKIDWNKILSYKIGKEMQNA
S. cerevisiae	- - - - VCT I RDI ETNFENDLDLSFF DLN EKQ FKA LRRQ LPVTR SKINWGSAIGSYRLGKNAAEGK
S. pombe	- - - - KLYEVLAQV ENGIQQSFNVELSS LND KKKFKE LRRQ LPVTR QKINWENVSGIRMRNT

B

	1
AtCPB	MEA AL GL L RRM PP KQSETA L SALLS L I PQHSSD LL SQVD L PL QVLRDIESGK-DFIL CEYNRD AD SYRS PWSNKY
Chicken B1	MS DQQLDCALD L MRR L PPQQIEKN L S DL ID L VP SLCED LL SS V D QP L KIARDKVVGK-DY LL C DYNRD GD SYRS PWSNKY
S. cerevisiae	MS DAQFDAAL D LL RR L NPTTLQEN L NN L IELQP N LAQD LL SSVD V PL S TQKDSADSNRE Y L CC DYNRD I DSFRS PWSNTY
S. pombe	MN SEDA AL D LL RR L NPKDISKN L DTILSVAP D LADV LL SSVD QP L KVNTCSESGN-QY LL C DFNRD GD SYRS PWSNKY

AtCPB	L PP L - - - - - ED ALYPSSE L RKLE VEAN D IFAIYRDQYYEGG I SSVYMWEDDNEG - - - - FVACF LI KKDGSKS GH GRRGC
Chicken B1	D PP L - - - - - ED GAMPSAR L RKLE VEANNAFDQYRDLYFEGG V SSVYL WDLDHG - - - - - - FAGV IL IKKAGDGS KK - - -
S. cerevisiae	Y PE LS PKDL Q D SPFPSAR L RKLE I LAND S FDVYRDLYYEGG I SSVYL WDLNEED FNGHD FAGVV LF KKNQS - - -
S. pombe	D PP L - - - - - ED GLVSTDRV RKLE VSLNEAIRVY LD LYYEGG V SSVYL WDQDDS - - - - - YAGAV IL KKASTS - - - - -

AtCPB	LE EGA WD AI HVI QVGSEEEE - -MAQY C LTS TI M LS L T TDDESS - - - - - GKF GLSG S IR RQ MKMELAVADG - - - - - - - H
Chicken B1	- IKG C WD SI HVV EVQEKSSG-RTAH Y K LTS TV M LW L Q TNKTGS - - - - GTMNL GGS LTRQ MEKDETVSDS - - - - - - - - SP H
S. cerevisiae	- DHSN WD SI HVF EVTTSPSS P DSF N YRV T T TI I LH L DKTKTDQ - - - - NSHMML SGN LTRQ TEKDIAIDMS RPLDVIF T SH
S. pombe	- NSSG WD SI HVF ECLPTTET-NVVD Y R LTS TI I LF L SSGSEEQ SALPS KALN L SGH LTRQ TSQRLPAADD - - - - - - - DTE

		256
AtCPB	L C NMGR MI EE L EGK L RNS L DQVYFGKT REMVCTLRPPAEIVQMRLPDT
Chicken B1	I AN I GR LVE D MENK I RS TL NE I YFGKT KDIVNGLRLSIDAIPDNQK-YKQLQREL SQV LT QR QIYIQPDN
S. cerevisiae	V AN LGS LIE DI ES QMRNLLETVYFEKT KDIFHQTKNAAIASSAEEANKDAQAEVIRGL QS L
S. pombe	I AN V GK LVE EM ET RMRNFLQDVYFGKT KDIINQTRSIQPVSDAQP-NDSALRSVLNDLLS I

FIG. 1. **Comparison of AtCP protein sequences with other heterodimeric capping proteins.** *A*, AtCPA and capping protein α subunits. *B*, AtCPB and capping protein β subunits. The gene accession numbers of capping protein subunits used for alignment are as follows: AtCPA (NM_111425); AtCPB (NM_105837); *S. cerevisiae* α (X61398); *S. cerevisiae* β (NC_001141); *S. pombe* α (Z70721); *S. pombe* β (AL391713); chicken α1 (M25534); chicken β1 (J04959); *O. sativa* α (*OsCPA*; AP005247.2). Secondary structure predictions are according to the crystal structure for the CapZ α1/β1 heterodimer from chicken muscle (21), with *solid cylinders* representing α-helices, and *dashed overlines* represent β-sheets. Alignments were prepared with the ClustalW algorithm in MacVector v.7.1.1 software (Accelrys, Madison WI). Gaps (−) were introduced to optimize the alignment, and residues that are conserved in 80% of the sequences are *highlighted*.

co-expressed in *E. coli* from a single T7 vector. A bacterial extract (Fig. 2*A*, *lane 1*) was fractionated with ammonium sulfate precipitation (Fig. 2*A*, *lane 2*) followed by chromatography on DEAE-Sephacel (Fig. 2*A*, *lane 3*), hydroxylapatite (Fig. 2*A*, *lane 4*), and Q-Sepharose (Fig. 2*A*, *lane 5*). After elution from Q-Sepharose, two major proteins of 38.8 and 30.8 kDa were evident, and these were typically present at a 1:1 stoichiometry. Purified AtCP was free of high molecular weight contaminants, but there was a small amount (5–10% of total protein) of two polypeptides that migrate between AtCPA and AtCPB. These are likely degradation products of AtCPA, as confirmed by Western blotting.

Immunoblots of *Arabidopsis* total seedling extracts and purified recombinant AtCP with affinity-purified anti-AtCPA antibody (Fig. 2*B*, *lanes 1* and *2*) and AtCPB antibody (Fig. 2*B*, *lanes 3* and *4*) were performed. The AtCPA antibody recognized one major polypeptide at the appropriate position for AtCP on purified recombinant protein (Fig. 2*B*, *lane 1*). AtCPA antibody also recognized minor, low molecular weight bands, suggesting that these are degradation products of the α subunit. AtCPA antibody detected one major band of ~39 kDa in *Arabidopsis* extracts (Fig. 2*B*, *lane 2*). Affinity-purified antibody specifically recognized AtCPB in the purified recombinant protein fraction (Fig. 2*B*, *lane 3*) and one band of ~31 kDa in *Arabidopsis* seedling total extracts (Fig. 2*B*, *lane 4*). These results demonstrate the presence of capping protein in plant tissues and

validate the specificity of the affinity-purified polyclonal antibodies.

AtCP Shifts the Critical Concentration for Actin Assembly—The effect of capping protein on the critical concentration (C_c) for actin assembly at steady state in the presence of 100 nM AtCP and 100 nM CapZ was determined. In these experiments, the C_c is taken as the *x* axis intercept from a plot of fluorescence from pyrene actin *versus* total actin concentration. A representative example of the effect of capping protein on C_c is shown in Fig. 3. 100 nM CapZ shifted the C_c from 0.16 μM (absence of capping protein) to 0.59 μM, in agreement with capping protein blocking assembly from the barbed or plus end. The accepted value for C_c at the pointed or minus ends of rabbit muscle Mg-ATP-actin is 0.6 μM (46). In the presence of 100 nM AtCP the C_c is 0.45 μM, close to the C_c at the pointed end.

AtCP Has Nucleation Activity—Many capping proteins have the ability to eliminate the lag period during actin assembly from monomers or nucleate filament formation (16, 17). Experiments to examine the effect of AtCP on the kinetics of rabbit muscle actin polymerization were performed. The results show that the initial lag corresponding to the nucleation step decreased with increasing AtCP concentration (Fig. 4*A*). Similar results were obtained with mouse CapZ (Fig. 4*B*), albeit with lower concentrations of capping protein required to achieve the same effect. Both sources of capping protein, at substoichiometric ratios to actin monomer, also enhanced the spontaneous

FIG. 2. **AtCP antibodies recognize recombinant and native proteins from *Arabidopsis*.** *A*, Coomassie Blue-stained protein gel of recombinant AtCP purification. *Lane 1*, total extract from bacterial cells (20 μg); *lane 2*, $(NH_4)_2SO_4$ precipitate (15 μg); *lane 3*, DEAE-Sephacel eluate (5 μg); *lane 4*, hydroxylapatite eluate (5 μg); *lane 5*, Q-Sepharose eluate (5 μg); *lane 6*, *A. thaliana* total seedling extract (25 μg). *B*, protein immunoblots probed with affinity-purified anti-CPA (*lanes 1* and *2*) and anti-CPB (*lanes 3* and *4*) antibodies. *Lanes 1* and *3* contain 1 μg of recombinant AtCP; *lanes 2* and *4* contain 30 μg of *A. thaliana* total seedling extract.
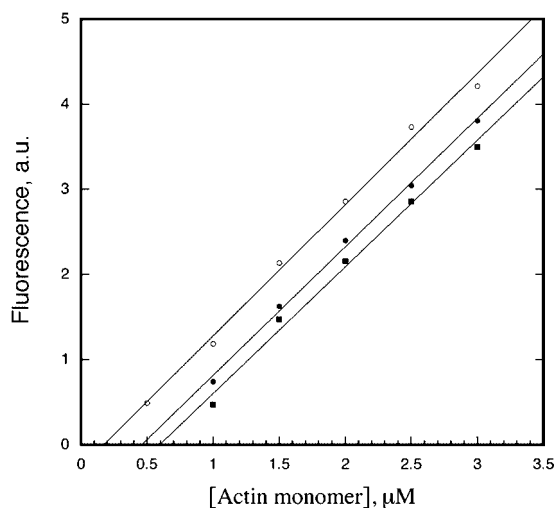
FIG. 3. **Capping protein shifts the critical concentration (C_c) to the value for pointed-end assembly.** Increasing concentrations of actin were incubated in the absence (*open circles*) or presence of 100 nM AtCP (*closed circles*) or 100 nM CapZ (*closed squares*) and allowed to polymerize for 16 h at room temperature. The C_c values (*x* axis intercept of each regression line) for this representative experiment were 0.16 μM for actin alone, 0.45 μM for AtCP, and 0.59 μM for CapZ. The experiment shows that AtCP and CapZ shift the steady-state C_c values for actin assembly. *a.u.*, arbitrary units.

assembly by creating new filament ends for growth.

The number of ends generated during these nucleation experiments was calculated from the slope at half-polymerization according to Equation 1. The efficiency of nucleation is then deduced from the ratio between the number of ends and the concentration of capping proteins. The highest efficiency of nucleation was obtained at low concentrations of capping proteins, with a maximum number of pointed ends of 0.17 for each CapZ molecule and 0.042 pointed ends for each AtCP molecule. These data are in agreement with Kovar *et al.* (47).

The calculation of the number of actin filaments also allowed
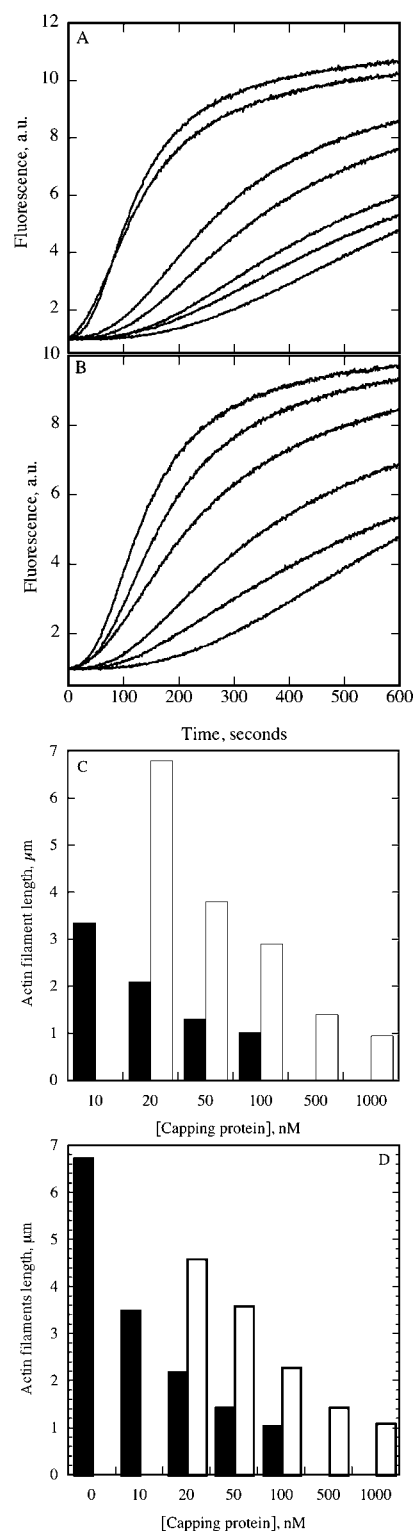
FIG. 4. **AtCP nucleates actin filament assembly.** AtCP and CapZ at various concentrations were incubated for 5 min with 2 μM actin (5% pyrene-labeled) before polymerization. Pyrene fluorescence is plotted *versus* time after the addition of KMEI buffer to initiate polymerization. The plots shown are from a single representative experiment (*n* = 3). *A*, AtCP at various concentrations, from *bottom* to *top*: 0, 10, 20, 50, 100, 500, and 1000 nM. *a.u.*, arbitrary units. *B*, CapZ at various concentrations, from *bottom* to the *top*: 0, 1, 2, 5, 10, and 50 nM. *C*, theoretical length distribution of actin filaments was calculated from the data shown in *A* and *B* using Equation 1 (see "Experimental Procedures"). *Black bars*, CapZ; *white bars*, AtCP. *D*, the actual length distribution of actin filaments as a function of AtCP (*white bars*) or CapZ (*black bars*) concentration is shown. Filament lengths were measured with MetaMorph from images such as those shown in Fig. 8. Mean values were obtained from 200 filaments at each concentration.
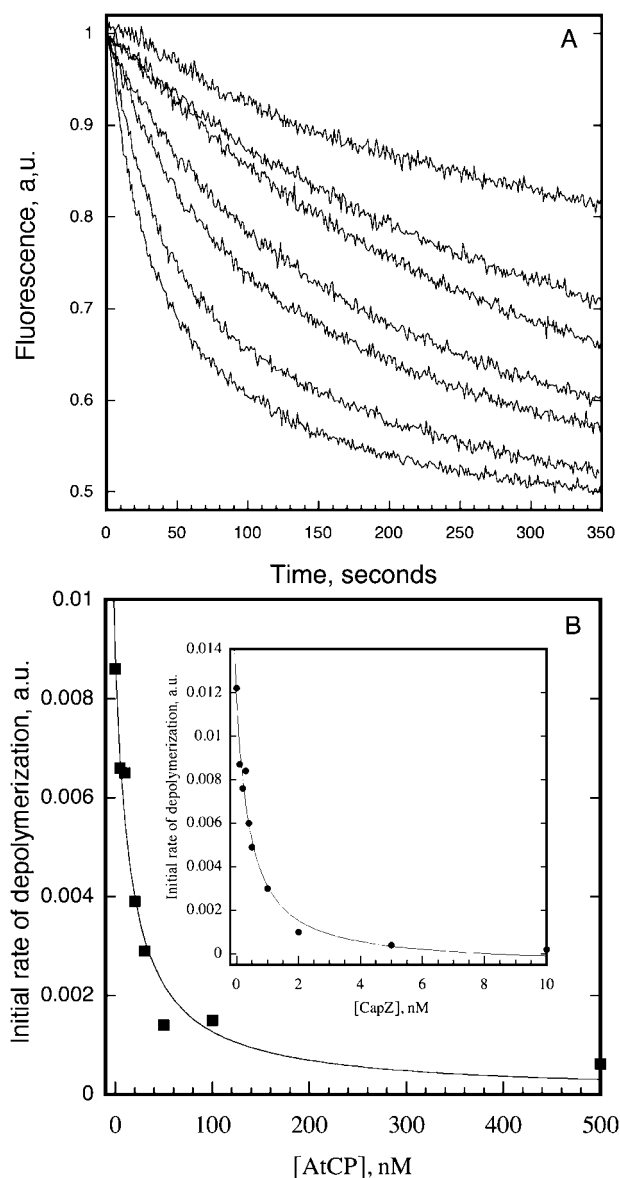
FIG. 5. **Capping protein inhibits actin filament depolymeriza-tion.** Capping proteins were incubated with 5 μM F-actin for 5 min before dilution of the solution 25-fold into Buffer G. *A*, depolymerization of F-actin in the presence of different AtCP concentrations, from *bottom* to *top*: 0, 10, 20, 30, 50, 100, and 500 nM. A representative experiment ($n = 3$) is shown. *B*, initial depolymerization rate *versus* AtCP and CapZ (*inset*) concentration from the data in A were plotted. The data were fit with Equation 2 ("Experimental Procedures") to determine dissociation equilibrium constant values of 16.7 nM for AtCP and 0.43 nM for CapZ. *a.u.*, arbitrary units.

us to predict the mean lengths of filaments in the presence of varying concentrations of capping protein, assuming that 1 μm of F-actin is composed of 334 actin subunits (13), using Equation 4.

$$\text{Length} = [\text{actin monomers}]/[\text{ends}] \qquad (\text{Eq. 4})$$

As shown in Fig. 4*C*, increasing amounts of capping protein correlate with decreased filament length, with AtCP less potent than CapZ. It seems likely that filament length would be reduced in such experiments by CP nucleating a large number of new filaments at high concentrations, thereby consuming the supply of actin subunits for assembly.

AtCP Prevents Depolymerization—The activity of capping protein was also measured with a depolymerization assay. The influence of capping protein on depolymerization was investi-

gated by diluting solutions of pyrene-labeled F-actin into Buffer G and monitoring the decrease in fluorescence. With increasing concentrations of AtCP, a significantly slower decrease in fluorescence was observed (Fig. 5*A*). Similar experiments performed with CapZ demonstrate the same relationship (not shown). These results indicate that AtCP can bind and block the depolymerization from the barbed ends of actin filaments. By fitting such data with Equation 2 we calculated mean K_d values ($\pm$S.D.; $n = 3$) of 12.2 $\pm$ 3.2 nM for AtCP and 0.3 $\pm$ 0.15 nM for CapZ (see Fig. 5*B* for representative experiments). This value for mouse CapZ is consistent with published values, ranging from 0.06 to 0.5 nM for capping protein from vertebrate muscle (24, 41, 48). For comparison, non-muscle and lower eukaryotic capping proteins have K_d values of 0.8–5 nM (24, 49–52).

Capping Protein Lowers the Rate of F-actin Elongation—The activity of capping protein was also tested kinetically with an elongation assay from F-actin seeds. The elongation rate depends on the availability of barbed ends under the following experimental conditions. 0.4 μM preformed F-actin seeds were incubated with varying concentrations of capping proteins for 5 min, and polymerization was initiated with addition of 1 μM G-actin (5% pyrene-labeled). The G-actin was saturated with 4 μM human profilin to prevent polymerization from pointed ends. The results show that the initial elongation rate was decreased with substoichiometric amounts of AtCP (Fig. 6*A*). Similar results were obtained for CapZ (not shown). By fitting the data to Equation 2, a K_d value of 20.1 nM was calculated (Fig. 6*B*). For comparison, a representative experiment for CapZ gave a K_d of 0.19 nM (Fig. 6*B*). From three such experiments, a mean K_d value ($\pm$S.D.) of 18.1 $\pm$ 3.9 nM for AtCP binding to rabbit muscle actin filaments was calculated. Elongation assays to determine the K_d of AtCP for *Zea mays* pollen actin were also performed. The mean K_d of 17.4 $\pm$ 5.4 nM ($n = 3$) was not significantly different when compared with rabbit muscle actin, demonstrating that AtCP does not have a preference for the source of actin.

To examine whether AtCP activity is regulated by calcium we performed identical elongation experiments in polymerization buffer supplemented with 1 mM EGTA and variable amounts of Ca^{2+}. Free Ca^{2+} concentrations of 200 nM to 200 μM had no obvious effect on the affinity of AtCP for barbed ends of filaments (Table I). For AtCP binding to rabbit skeletal muscle actin, a K_d value of 26.4 μM at 200 μM free Ca^{2+} was not significantly different from the K_d of 21.1 nM at 200 nM Ca^{2+}. Thus, *Arabidopsis* capping protein appears to be relatively insensitive to calcium levels.

Steady-state Determination—We also determined the dissociation constant (K_d) for binding of capping protein to F-actin by measuring the ability to alter the C_c for actin polymerization at equilibrium. From the data in Fig. 7, the apparent critical concentration is shifted half-maximally at about 26.3 nM for AtCP and 1.8 nM for CapZ. From three similar experiments, a mean K_d value ($\pm$S.D.) of 23.6 $\pm$ 14.2 nM for AtCP was obtained. Therefore, AtCP has an apparent K_d for filament barbed ends, as determined during dynamic polymerization/depolymerization or at equilibrium, of 12–24 nM.

Effects of AtCP on Actin Filament Length—Fluorescence microscopy was used to determine the effect of capping protein on the length distribution of actin filaments. When 4 μM actin was polymerized in the presence of an equimolar amount of rhodamine-phalloidin and diluted to a final concentration of 10 nM before attaching to polylysine-coated coverslips, the number of filaments per field was few, and their length distribution was approximately exponential (Fig. 8*A*; mean of 6.74 $\pm$ 4.6 μm). By contrast, when actin was polymerized in the presence of 200 nM
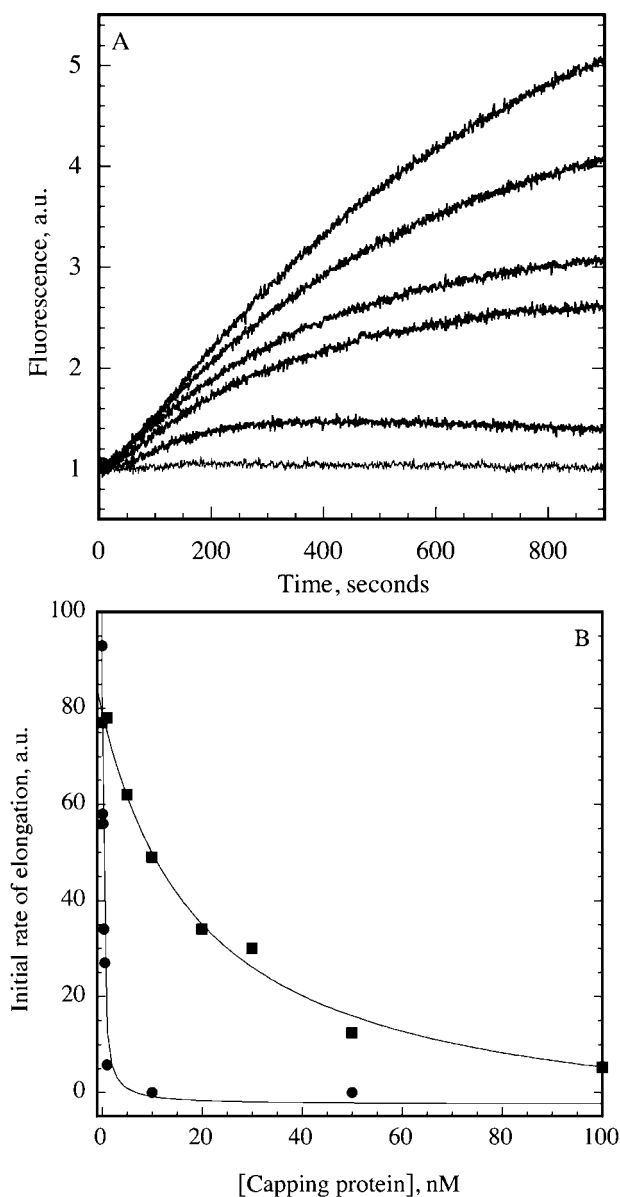
FIG. 6. **AtCP inhibits elongation at barbed ends of actin filaments.** *A*, preformed F-actin (0.4 μM) seeds were incubated with different concentrations of AtCP, and 1 μM G-actin saturated with 4 μM human profilin I was added to initiate actin elongation at the barbed end. The change in pyrene-actin fluorescence accompanying polymerization is plotted *versus* time after addition of G-actin. From *bottom* to *top*, AtCP concentration is 150, 50, 30, 20, 10, and 0 nM. A single representative experiment (*n* = 3) is shown. *B*, initial rates of elongation *versus* AtCP (*closed squares*) and CapZ (*closed circles*) concentration were plotted for the representative experiment shown in *A*. The data were fit with Equation 2 ("Experimental Procedures") to determine predicted dissociation equilibrium constant values of 20.1 nM for AtCP and 0.19 nM for CapZ.

TABLE I
AtCP binding to filament barbed ends is calcium independent

Free Ca^{2+a}	$K_d \pm$ S.D.^{b}	n^c	R value^d
	nM		
200 nM	21.1 $\pm$ 5.0	7	0.990
2 μM	21.9 $\pm$ 5.1	5	0.997
20 μM	23.4 $\pm$ 4.9	6	0.995
200 μM	26.4 $\pm$ 8.1	6	0.989

^{a} Free calcium concentration in the presence of 1.12 mM EGTA was calculated using the EGTA program.

^{b} Mean K_d values (in nM) for binding to filament barbed ends from a representative experiment ($\pm$S.D.) of the elongation assay performed at different free calcium levels are given.

^{c} Sample size (*n*) for these experiments is the number of AtCP concentrations used to determine a K_d value.

^{d} *R* value for deviation of datapoints from the line of best fit according to Equation 2 ("Experimental Procedures").
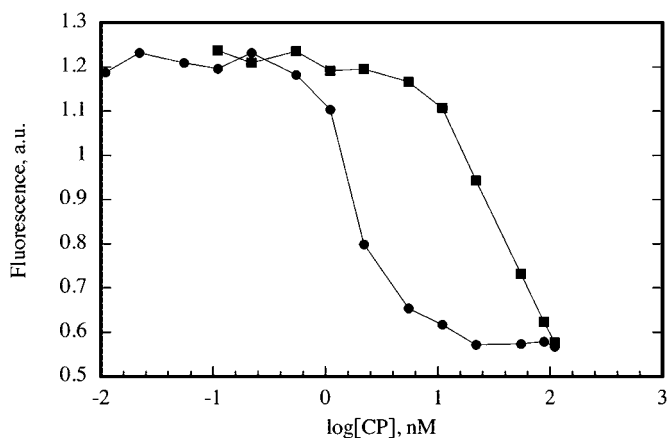
FIG. 7. **AtCP has a high affinity for filament ends.** In addition to the dynamic assembly and disassembly assays described above, the affinity of capping protein for filament ends was determined at steady state. Actin at 1 μM was incubated with various concentrations of AtCP or CapZ in 1× KMEI buffer for 24 h. Fluorescence of pyrene-actin *versus* the log of the capping protein concentration for a single, representative experiment for CapZ (*closed circles*) and AtCP (*closed squares*) is plotted. The K_d for capping protein binding to actin was determined from the amount of capping protein that changes the critical concentration by 50% (24). For these representative experiments, the predicted K_d was 26.3 nM for AtCP and 1.77 nM for CapZ.

loidin. As a control, when both ends are free Alexa-488 phalloidin-labeled actin elongated from both ends of red actin filaments (Fig. 8*D*). There is also some contribution of annealing to filament length during these reactions, since a small number of green filaments with a short stretch of red filament are also observed. In the presence of saturating amounts of CapZ (Fig. 8*E*) or AtCP (Fig. 8*F*), green actin filaments grew almost exclusively from one end of the red actin seeds. Moreover, the extent of green actin filament growth was short, suggesting that capping protein blocked all available barbed ends, and green actin filaments extended only from pointed ends.

The length distribution of actin filaments as a function of capping protein function was determined directly from fluorescence micrographs (Fig. 4*D*). The actual mean length from microscopy correlates well with the predicted length calculated from nucleation experiments (Fig. 4*C*). For example, the predicted mean length of actin filaments in the presence of 100 nM AtCP was 2.92 μm, and the actual value was 2.27 $\pm$ 2.0 μm. For CapZ at 100 nM, predicted and actual mean lengths were 1.02 and 1.05 $\pm$ 1.03 μm, respectively. This confirms that the presence of rhodamine phalloidin or Alexa-488 phalloidin has no influence on the length of actin filaments observed during fluorescence microscopy experiments.

The ability of capping proteins to bind and block the activity of barbed ends was tested further with filament annealing
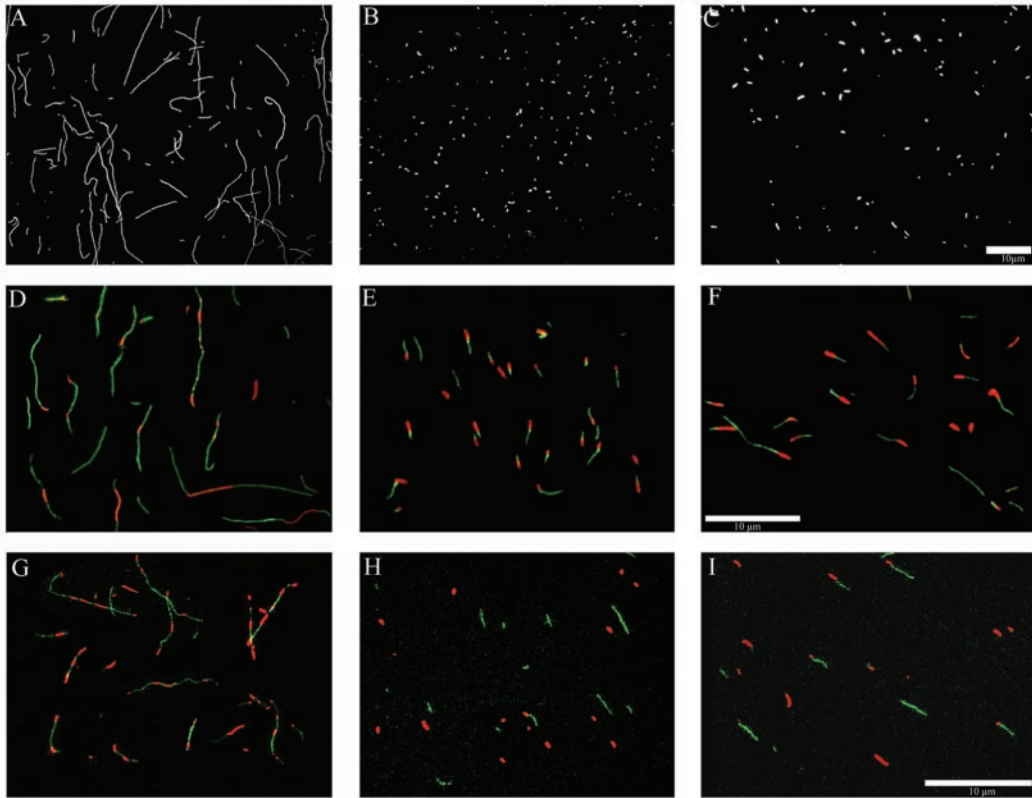
CapZ (Fig. 8*B*) or 500 nM AtCP (Fig. 8*C*), the mean length of filaments (0.76 $\pm$ 0.73 and 1.45 $\pm$ 1.3 μm, respectively) was reduced substantially, and the length distribution was quite uniform. The results are consistent with capping protein nucleating actin filament formation and increasing the number of actin filaments.

We confirmed that the barbed ends of actin filaments are blocked by capping proteins using a fluorescence microscopy assay (43). Actin filaments generated as described above were used as prelabeled templates or seeds (*red*) for subsequent elongation. Newly elongated actin filaments are green because the elongation is performed in the presence of Alexa-488 phal-

FIG. 8. **Capping protein reduces the length of actin filaments and allows growth from only one end.** Fluorescence micrographs of individual actin filaments assembled in the presence or absence of capping proteins are shown. The *scale bars* represent 10 μm *A–C*, the effect of capping protein on filament length is shown. In each case 4 μM Mg-ATP-actin was polymerized for 30 min in the presence of 4 μM rhodamine-phalloidin. *A*, actin filaments formed in the absence of capping protein. *B*, 200 nM CapZ. *C*, 500 nM AtCP. *D–F*, two-color overlays of actin filament assembly from rhodamine-phalloidin labeled actin seeds (*red*). The new growth is marked by Alexa-488 phalloidin (*green*). *D*, 2 μM actin seeds stabilized with rhodamine-phalloidin were incubated with 1 μM Mg-ATP-actin for 15 min in the presence of 1 μM Alexa-488 phalloidin. Because the filament density was much lower, due to the increased filament length at equivalent actin concentrations to those shown in *E* and *F*, this image is a montage created from 6 different fields. *E*, CapZ-capped seeds (0.5 μM) labeled with rhodamine-phalloidin were used for new polymerization as described for *D*. *F*, AtCP-capped seeds (0.5 μM). *G–I*, actin filament annealing in the presence of capping protein was examined by total internal reflectance fluorescence microscopy. Populations of red or green actin filament, 2 μM each, were sheared by sonication and incubated together in the presence or absence of capping proteins. Dual color images were created after at least 60 min of incubation. Capping protein inhibits filament annealing. *G*, actin in the absence of capping protein. *H*, 200 nM CapZ. *I*, 500 nM AtCP

reactions. Populations of red- and green-actin filaments (2 μM each) were sheared by sonication in the presence or absence of capping protein at saturating concentrations and allowed to incubate. After more than 60 min filaments were examined by total internal reflectance fluorescence microscopy, and dual-color images were generated. In the absence of capping protein long filaments composed of interspersed stretches of red and green polymer were observed frequently (Fig. 8*G*). In this experiment populations of annealed filaments had a mean length of 3.45 $\pm$ 2.66 μm. In the presence of 200 nM Cap Z or 500 nM AtCP, very few dual color filaments were present in the populations, and the mean length of filaments was quite short, 0.81 and 0.9 μm, respectively. This provides additional confirmation that AtCP blocks the availability of filament barbed ends, as shown previously for CapZ by Kovar *et al.* (47).

Effect of PtdIns(4,5)P₂ on Capping Protein Activity—To test the potential regulation of AtCP, the effect of PtdIns(4,5)P$_2$ on capping protein activity with elongation and depolymerization assays was examined. During elongation from actin seeds, 5 nM CapZ inhibited actin assembly almost completely (Fig. 9*A*). In the presence of 5 μM PtdIns(4,5)P$_2$ in micellar form, however, the rate of initial actin assembly was equivalent to actin alone. To inhibit actin assembly completely under these conditions required 100 nM AtCP (Fig. 9*B*). A 1000:1 ratio of phospholipid to capping protein, or 100 μM PtdIns(4,5)P$_2$, only restored the initial rate of actin assembly partially. During the depolymerization assay, a 1000-fold excess of phospholipid completely

abolished the activity of CapZ (Fig. 9*D*) but only partially inhibited the activity of AtCP (Fig. 9*C*). Thus, PtdIns(4,5)P$_2$ can regulate the activity of AtCP, but the binding of AtCP to phospholipid is likely to have a lower affinity than does CapZ.

DISCUSSION

Here we report the first molecular and biochemical characterization of a capping protein from higher plants. Recombinant *A. thaliana* capping protein, AtCP, is an α/β heterodimer of 39- and 31-kDa subunits when co-expressed in bacterial cells and purified by multiple chromatography steps. Like other members of this ubiquitous class of ABPs, AtCP binds to filament ends with high affinity and prevents actin polymerization and depolymerization. During actin polymerization, AtCP is an efficient nucleator of actin filament formation from monomers and reduces the lag period before actin assembly. Its activity is not regulated by calcium but is moderately sensitive to the signaling lipid PtdIns(4,5)P$_2$. The ability of AtCP to bind vertebrate muscle actin was compared with plant actin, and no preference for isoform was observed; therefore, the bulk of quantitative assays reported here was performed with muscle actin.

The affinity of capping proteins for the barbed end of filaments was examined at steady state as well as during assembly or disassembly. AtCP prevented the addition of profilin-actin complex to barbed ends of filaments and inhibited dilution-mediated depolymerization. At equilibrium, substoichiometric
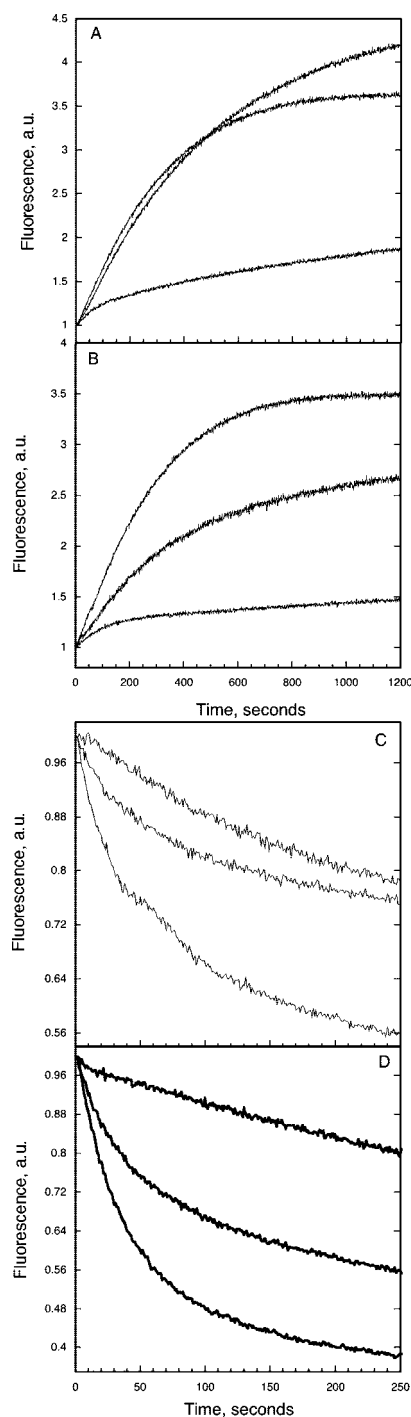
Arabidopsis Capping Protein

FIG. 9. **AtCP activity is inhibited by phosphoinositide lipids.** Actin elongation assays, similar to those in Fig. 6, were performed in the presence of capping protein with and without PtdIns(4,5)P$_2$ micelles. *A*, CapZ. From *bottom* to *top*, the curves represent 1 μM actin plus 5 nM CapZ, 1 μM actin alone, and 1 μM actin plus 5 nM CapZ plus 5 μM PtdIns(4,5)P$_2$. *B*, AtCP. From *bottom* to *top*, the curves represent 1 μM actin plus 100 nM AtCP, 1 μM actin plus 100 nM CapZ plus 100 μM PtdIns(4,5)P$_2$, and 1 μM actin alone. Actin depolymerization assays, similar to those in Fig. 5, were performed in the presence of capping protein with and without PtdIns(4,5)P$_2$ micelles. *C*, AtCP. From *bottom* to *top*, the curves represent 5 μM actin only, 5 μM actin plus 100 μM AtCP plus 2 μM PtdIns(4,5)P$_2$, and 5 μM actin plus 100 nM AtCP. *D*, CapZ. From *bottom* to *top*, the curves represent 5 μM actin only, 5 μM actin plus 2 nM CapZ plus 2 μM PtdIns(4,5)P$_2$, and 5 μM actin plus 2 nM CapZ.

amounts of AtCP shifted the critical concentration for assembly to a value near that of the pointed end and caused a dose-dependent reduction in the amount of polymer formed. The ob-

served K_d values calculated from these assays, ranging from 12–24 nM, are somewhat higher than those found in the literature for vertebrate muscle CapZ (24, 41, 48, 53) or in our direct comparisons with mouse CapZ (K_d 0.19–1.8 nM). However, they are not too different from non-muscle capping protein (1–5 nM; Refs. 49–52 and 54) or recombinant *Schizosaccharomyces pombe* CP.[2] Lack of conservation of the primary amino acid sequence at the C termini of both subunits may account for these differences in affinity, ability to nucleate, and/or on- and off-rates for capping (44). The crystal structure of chicken CapZ ($\alpha 1\beta 1$) demonstrates that the C termini are amphipathic helices that probably form contacts with two separate actin monomers (21). This interpretation is consistent with earlier experimental evidence demonstrating the importance of the C terminus from the β-subunit (44, 45, 48, 53).

In addition to binding barbed ends with high affinity, AtCP nucleates filament assembly from monomers and stimulates initial polymerization rates *in vitro*. Although capping proteins from vertebrate muscle (41) and *Acanthamoeba* (17) can nucleate filament formation, a few, like human polymorphonuclear leukocyte CapZ (51), *Dictyostelium* cap32/34 (54, 55), and *S. pombe* CP,[2] lack this activity. The efficiency of nucleation, which is only 4-fold different between AtCP and mouse CapZ, suggests that the nearly 100-fold difference in apparent K_d for barbed ends is not simply a consequence of large amounts of dead or denatured protein in our AtCP preparations. ABPs like villin, adseverin, and gelsolin can also sever actin filaments along their backbone, creating new ends for subunit loss or addition. AtCP does not appear to sever actin filaments; this would have been evident in the elongation and depolymerization assays as increased rates of assembly/disassembly. The ability to block subunit addition or loss at filament ends is confirmed by fluorescence light microscopy, where we find that AtCP causes a dose-dependent reduction in mean filament length and allows only small amounts of assembly from one end of pre-existing filament seeds, as shown previously for muscle CP (56). It also prevents the ability of actin filaments to anneal, which keeps the average filament length short in the presence of capping protein. AtCP is, therefore, an effective regulator of actin filament dynamics and assembly *in vitro*.

Other than a 75-kDa glycoprotein purified from *Impatiens* fruit pods (57), there is no prior evidence for capping protein activity in plants. This unidentified protein is an apparent homotetramer that inhibits actin polymerization in seeded elongation reactions. It also reduces filament length in the electron microscope and co-sediments with F-actin. However, because Hsc70, an abundant heat shock protein and chaperone, co-purifies and interacts with capping protein from *Dictyostelium* (54, 55) and the malarial parasite *Plasmodium* (58), the possibility that small amounts of CP are present and responsible for the activity in the purified 75-kDa ABP fractions from *Impatiens* cannot be excluded. Until molecular identification of this novel protein is achieved, our study on AtCP represents the first report of a *bona fide* capping protein from higher plants.

The function of capping proteins may depend on the organism, the stage of development, the repertoire of other ABPs, and the size and activity of the actin subunit pool in specific cells. During vertebrate muscle development, CapZ plays a critical role in the assembly of actin filaments that comprise the sarcomere (59). Null mutants of *Drosophila* show that CP is essential for viability (60), whereas *Saccharomyces cerevisiae* mutants for CP subunits are not lethal but show defects in growth, cellular polarity, F-actin levels, and cell wall deposition

---

[2] D. R. Kovar and T. D. Pollard, unpublished data.

(61–63). In *Dictyostelium*, over- and underexpression of CP alters agonist-induced cell motility (64). These phenotypes are a result of apparently opposite behavior of CP on F-actin levels or assembly in the different organisms and are consistent with CP function depending on other ABPs. Genetic studies demonstrate interactions between CP and profilin (65), fimbrin (66–68), and twinfilin (27). And biochemical analysis suggests that CP may compete with formin-homology proteins for the regulation of filament barbed ends (47).

We hypothesize that AtCP is a major regulator of filament turnover and F-actin levels in plant cells. In particular we predict that capping protein activity is responsible in part for the large amount of monomer actin in plant cells and that the majority of actin filament barbed ends are capped (69). As argued previously, this could explain the potent effect of profilin overexpression in interphase plant cells (10). In contrast to yeast, which contain rather low levels of total actin but a high proportion (~90%) of F-actin to monomer (63), plant pollen contains high levels of total actin and only a small amount present in filamentous form. Quantitative analysis of maize and poppy pollen indicates total cellular actin concentrations of 127–221 μM, similar to many vertebrate cells, but just 11–16 μM actin in polymer (33, 70). The predicted large actin subunit pool is probably buffered by a roughly equimolar pool (125–194 μM) of profilin (33, 70), which should elongate any existing actin filaments from the barbed end until capping occurs (47, 71, 72), then profilin will act as a simple sequestering protein and will suppress spontaneous actin filament nucleation. Therefore, the combination of profilin and CP in pollen will serve to maintain a large pool of actin subunits, which could be used for actin elongation at free barbed ends. Biochemical data from other systems show that the combination of CP and profilin increase the density of branched networks generated by the Arp2/3 complex (43) and are consistent with CP functioning to sustain a large pool of actin subunits. Cellular concentrations of CP often correlate with numbers of filament ends such that all filament ends are thought to be capped (50, 51). If a similar situation exists in plants with [CP] in the low μM range, then the expectation is that average filament lengths should depend on the extent of capping. The size of actin filaments will be further ensured by the ability of CP to prevent actin filament annealing. Accurate measurements of [CP] in plants and subcellular localization are urgently needed.

Like many classes of ABP (73), capping protein may be a stimulus-responsive regulator of actin organization. The actin-binding activity of CP from vertebrate muscle, human erythrocytes, *Dictyostelium*, and yeast is reduced or eliminated in the presence of the membrane phosphoinositide lipid, phosphatidylinositol 4,5-bisphosphate (22–24, 45, 51, 52, 74). AtCP binding to actin filament barbed ends is also inhibited by PtdIns(4,5)P$_2$ but is insensitive to calcium. The phospholipid binding site on CP has not been determined but likely overlaps with the actin binding residues (21, 45). Moreover, like other plant ABPs (6, 10, 75), the affinity of AtCP for PtdIns(4,5)P$_2$ appears to be somewhat lower than that for vertebrate ABPs. Measuring the K_d for phospholipid directly and examination of the ability of AtCP to bind 3-phosphorylated phosphoinositides should be attempted. It is also possible that protein-protein interactions modulate capping protein function. In other systems, capping protein binds to the myosin I and Arp2/3 complex-interacting protein CARMIL (28), the V-1 protein (29), Arp1 minifilaments that are part dynactin complex (30), the ADF/cofilin-related protein, twinfilin (27), and Hsc70 (49, 54, 55, 58, 76). Only the V-1 protein or myotrophin, which is composed of three consecutive ankyrin repeats only, appears to alter the activity of CP (29). The *Arabidopsis* genome does not

contain obvious orthologues of Arp1, CARMIL, or twinfilin (8, 77)[3]; however, numerous ankyrin-repeat proteins are present, and these should be tested for direct interactions with AtCP.

REFERENCES

1. Vantard, M., and Blanchoin, L. (2002) *Curr. Opin. Plant Biol.* **5,** 502–506
2. Kreis, T., and Vale, R. (1999) *Guidebook to the Cytoskeletal and Motor Proteins*, 2nd Ed., Oxford University Press, New York
3. Pollard, T. D., and Borisy, G. G. (2003) *Cell* **112,** 453–465
4. Staiger, C. J., and Hussey, P. J. (2003) in *The Plant Cytoskeleton in Cell Differentiation and Development* (Hussey, P. J., ed) pp. 32–80, Blackwell Publishers, UK
5. Wasteneys, G. O., and Galway, M. E. (2003) *Annu. Rev. Plant Biol.* **54,** 691–722
6. Kovar, D. R., Yang, P., Sale, W. S., Drøbak, B. K., and Staiger, C. J. (2001) *J. Cell Sci.* **114,** 4293–4305
7. Kashiyama, T., Kimura, N., Mimura, T., and Yamamoto, K. (2000) *J. Biochem. (Tokyo)* **127,** 1065–1070
8. Hussey, P. J., Allwood, E. G., and Smertenko, A. P. (2002) *Philos. Trans. R. Soc. Lond. B. Biol. Sci.* **357,** 791–798
9. Meagher, R. B., McKinney, E. C., and Kandasamy, M. K. (1999) *Plant Cell* **11,** 995–1005
10. Kovar, D. R., Drøbak, B. K., and Staiger, C. J. (2000) *Plant Cell* **12,** 583–598
11. Allwood, E. G., Anthony, R. G., Smertenko, A. P., Reichelt, S., Drøbak, B. K., Doonan, J. H., Weeds, A. G., and Hussey, P. J. (2002) *Plant Cell* **14,** 2915–2927
12. Loisel, T. P., Boujemaa, R., Pantaloni, D., and Carlier, M.-F. (1999) *Nature* **401,** 613–616
13. Pollard, T. D., Blanchoin, L., and Mullins, R. D. (2000) *Annu. Rev. Biophys. Biomol. Struct.* **29,** 545–576
14. Vignjevic, D., Yarar, D., Welch, M. D., Peloquin, J., Svitkina, T., and Borisy, G. G. (2003) *J. Cell Biol.* **160,** 951–962
15. Cooper, J. A., and Schafer, D. A. (2000) *Curr. Opin. Cell Biol.* **12,** 97–103
16. Cooper, J. A., Hart, M. C., Karpova, T. S., and Schafer, D. A. (1999) in *Guidebook to the Cytoskeletal and Motor Proteins* (Kreis, T., and Vale, R., eds) 2nd Ed., pp. 62–64, Oxford University Press, NY
17. Isenberg, G., Aebi, U., and Pollard, T. D. (1980) *Nature* **288,** 455–459
18. Casella, J. F., Maack, D. J., and Lin, S. (1986) *J. Biol. Chem.* **261,** 10915–10921
19. Pantaloni, D., Boujemaa, R., Didry, D., Gounon, P., and Carlier, M.-F. (2000) *Nat. Cell Biol.* **2,** 385–391
20. Wiesner, S., Helfer, E., Didry, D., Ducouret, G., Lafuma, F., Carlier, M.-F., and Pantaloni, D. (2003) *J. Cell Biol.* **160,** 387–398
21. Yamashita, A., Maeda, K., and Maéda, Y. (2003) *EMBO J.* **22,** 1529–1538
22. Heiss, S. G., and Cooper, J. A. (1991) *Biochemistry* **30,** 8753–8758
23. Haus, U., Hartmann, H., Trommler, P., Noegel, A. A., and Schleicher, M. (1991) *Biochem. Biophys. Res. Commun.* **181,** 833–839
24. Schafer, D. A., Jennings, P. B., and Cooper, J. A. (1996) *J. Cell Biol.* **135,** 169–179
25. Waddle, J. A., Karpova, T. S., Waterston, R. H., and Cooper, J. A. (1996) *J. Cell Biol.* **132,** 861–870
26. Schafer, D. A., Welch, M. D., Machesky, L. M., Bridgman, P. C., Meyer, S. M., and Cooper, J. A. (1998) *J. Cell Biol.* **143,** 1919–1930
27. Palmgren, S., Ojala, P. J., Wear, M. A., Cooper, J. A., and Lappalainen, P. (2001) *J. Cell Biol.* **155,** 251–260
28. Jung, G., Remmert, K., Wu, X. F., Volosky, J. M., and Hammer, J. A. I. (2001) *J. Cell Biol.* **153,** 1479–1497
29. Taoka, M., Ichimura, T., Wakamiya-Tsuruta, A., Kubota, Y., Araki, T., Obinata, T., and Isobe, T. (2003) *J. Biol. Chem.* **278,** 5864–5870
30. Schafer, D. A., Gill, S. R., Cooper, J. A., Heuser, J. E., and Schroer, T. A. (1994) *J. Cell Biol.* **126,** 403–412
31. Soeno, Y., Abe, H., Kimura, S., Maruyama, K., and Obinata, T. (1998) *J. Muscle Res. Cell Motil.* **19,** 639–646
32. Ren, H., Gibbon, B. C., Ashworth, S. L., Sherman, D. M., Yuan, M., and Staiger, C. J. (1997) *Plant Cell* **9,** 1445–1457
33. Gibbon, B. C., Kovar, D. R., and Staiger, C. J. (1999) *Plant Cell* **11,** 2349–2363
34. Kovar, D. R., Staiger, C. J., Weaver, E. A., and McCurdy, D. W. (2000) *Plant J.* **24,** 625–636
35. Tang, W.-J., (1993) *Methods Cell Biol.* **37,** 95–104
36. Spudich, J. A., and Watt, S. (1971) *J. Biol. Chem.* **246,** 4866–4871
37. Pollard, T. D. (1984) *J. Cell Biol.* **99,** 769–777
38. Houk, T. W., Jr., and Ue, K. (1974) *Anal. Biochem.* **62,** 66–74
39. Brenner, S. L., and Korn, E. D. (1983) *J. Biol. Chem.* **258,** 5013–5020
40. Pollard, T. D. (1986) *J. Cell Biol.* **103,** 2747–2754
41. Caldwell, J. E., Heiss, S. G., Mermall, V., and Cooper, J. A. (1989) *Biochemistry* **28,** 8506–8514
42. Walsh, T. P., Weber, A., Higgins, J., Bonder, E. M., and Mooseker, M. S. (1984) *Biochemistry* **23,** 2613–2621
43. Blanchoin, L., Pollard, T. D., and Mullins, R. D. (2000) *Curr. Biol.* **10,**

---

[3] C. J. Staiger and S. Huang, unpublished data.

1273–1282

44. Hug, C., Miller, T., Torres, M. A., Casella, J. F., and Cooper, J. A. (1992) *J. Cell Biol.* **116,** 923–931

45. Sizonenko, G. I., Karpova, T. S., Gattermeir, D. J., and Cooper, J. A. (1996) *Mol. Biol. Cell* **7,** 1–15

46. Sheterline, P., Clayton, J., and Sparrow, J. C. (1998) *Protein Profile* **4,** 1–272

47. Kovar, D. R., Kuhn, J. R., Tichy, A. L., and Pollard, T. D. (2003) *J. Cell Biol.* **161,** 875–887

48. Barron-Casella, E. A., Torres, M. A., Scherer, S. W., Heng, H. H. Q., Tsui, L.-C., and Casella, J. F. (1995) *J. Biol. Chem.* **270,** 21472–21479

49. Eddy, R. J., Han, J. H., Sauterer, R. A., and Condeelis, J. S. (1996) *Biochim. Biophys. Acta* **1314,** 247–259

50. DiNubile, M. J., Cassimeris, L., Joyce, M., and Zigmond, S. H. (1995) *Mol. Biol. Cell* **6,** 1659–1671

51. Maun, N. A., Speicher, D. W., DiNubile, M. J., and Southwick, F. S. (1996) *Biochemistry* **35,** 3518–3524

52. Kuhlman, P. A., and Fowler, V. M. (1997) *Biochemistry* **36,** 13461–13472

53. Casella, J. F., and Torres, M. A. (1994) *J. Biol. Chem.* **269,** 6992–6998

54. Sauterer, R. A., Eddy, R. J., Hall, A. L., and Condeelis, J. S. (1991) *J. Biol. Chem.* **266,** 24533–24539

55. Eddy, R. J., Sauterer, R. A., and Condeelis, J. S. (1993) *J. Biol. Chem.* **268,** 23267–23274

56. Xu, J., Casella, J. F., and Pollard, T. D. (1999) *Cell Motil. Cytoskeleton* **42,** 73–81

57. Pal, M., and Biswas, S. (1994) *Mol. Cell. Biochem.* **130,** 111–120

58. Tardieux, I., Baines, I., Mossakowska, M., and Ward, G. E. (1998) *Mol. Biochem. Parasitol.* **93,** 295–308

59. Schafer, D. A., Hug, C., and Cooper, J. A. (1995) *J. Cell Biol.* **128,** 61–70

60. Hopmann, R., Cooper, J. A., and Miller, K. G. (1996) *J. Cell Biol.* **133,** 1293–1305

61. Amatruda, J. F., Cannon, J. F., Tatchell, K., Hug, C., and Cooper, J. A. (1990) *Nature* **344,** 352–354

62. Amatruda, J. F., Gattermeir, D. J., Karpova, T. S., and Cooper, J. A. (1992) *J. Cell Biol.* **119,** 1151–1162

63. Karpova, T. S., Tatchell, K., and Cooper, J. A. (1995) *J. Cell Biol.* **131,** 1483–1493

64. Hug, C., Jay, P. Y., Reddy, I., McNally, J. G., Bridgman, P. C., Elson, E. L., and Cooper, J. A. (1995) *Cell* **81,** 591–600

65. Hopmann, R., and Miller, K. G. (2003) *Mol. Biol. Cell* **14,** 118–128

66. Karpova, T. S., Lepetit, M. M., and Cooper, J. A. (1993) *Genetics* **135,** 693–709

67. Adams, A. E. M., Cooper, J. A., and Drubin, D. G. (1993) *Mol. Biol. Cell* **4,** 459–468

68. Nakano, K., Satoh, K., Morimatsu, A., Ohnuma, M., and Mabuchi, I. (2001) *Mol. Biol. Cell* **12,** 3515–3526

69. Staiger, C. J., Gibbon, B. C., Kovar, D. R., and Zonia, L. E. (1997) *Trends Plant Sci.* **2,** 275–281

70. Snowman, B. N., Kovar, D. R., Shevchenko, G., Franklin-Tong, V. E., and Staiger, C. J. (2002) *Plant Cell* **14,** 2613–2626

71. Pantaloni, D., and Carlier, M.-F. (1993) *Cell* **75,** 1007–1014

72. Kang, F., Purich, D. L., and Southwick, F. S. (1999) *J. Biol. Chem.* **274,** 36963–36972

73. Yin, H. L., and Janmey, P. A. (2003) *Annu. Rev. Physiol.* **65,** 761–789

74. Amatruda, J. F., and Cooper, J. A. (1992) *J. Cell Biol.* **117,** 1067–1076

75. Gungabissoon, R. A., Jiang, C.-J., Drøbak, B. K., Maciver, S. K., and Hussey, P. J. (1998) *Plant J.* **16,** 689–696

76. Haus, U., Trommler, P., Fisher, P. R., Hartmann, H., Lottspeich, F., Noegel, A. A., and Schleicher, M. (1993) *EMBO J.* **12,** 3763–3771

77. McKinney, E. C., Kandasamy, M. K., and Meagher, R. B. (2002) *Plant Physiol.* **128,** 997–1007